Energy, Mines and Resources Canada | Énergie, Mines et Ressources Canada

CANMET

Canada Centre for Mineral and Energy Technology | Centre canadien de la technologie des minéraux et de l'énergie

THE BEHAVIOUR OF BUOYANT PLUMES FROM AN OIL-SANDS REFINERY COMPLEX

H. WHALEY AND G.K. LEE

CANADIAN COMBUSTION RESEARCH LABORATORY

APRIL 1977

For presentation at the Canada-Venezuela Oil Sands Symposium 77, Edmonton, Alberta, May 27 - June 4, 1977

ENERGY RESEARCH PROGRAM

ENERGY RESEARCH LABORATORIES

REPORT ERP/ERL 77-33 (OP) C.2

THE BEHAVIOUR OF BUOYANT PLUMES FROM AN OIL-SANDS REFINERY COMPLEX

by

H. Whaley* and G.K. Lee*

ABSTRACT

A plume dispersion research program using an instrumented helicopter was conducted at an oil-sands refinery complex in northern Alberta during the fall and winter. Atmospheric conditions ranged from stable to neutral in both seasons with an elevated inversion being present throughout the winter study period. Spatial SO_2 concentration and temperature profile measurements were used to derive dispersion parameters by numerical analysis.

The derived dispersion parameters have shown that presently accepted empirical formulae for predicting plume behaviour and plume impingement patterns on the ground cannot be applied with confidence in this region.

---

* Research Scientists, Canadian Combustion Research Laboratory, Energy Research Laboratories, Canada Centre for Mineral and Energy Technology, Department of Energy, Mines and Resources, Ottawa, Canada.

Nomenclature

C max	=	concentration on plume centreline, ppm
Cp	=	specific heat of air at constant pressure, $J/kg^{o}C$
E	=	emission rate of SO_2, sm^3/s
F	=	buoyancy flux = $gQ/\pi C_p \rho T$, m^4/s^3
g	=	gravitation constant, m/s^2
h	=	height of stack above ground, m
L	=	characteristic length for a buoyant plume = F/U^3, m
Q	=	heat emission from stack, J/s
S	=	stability parameter = $g/T\ (\partial\Theta/\partial z)$, s^{-2}
T	=	absolute temperature of ambient air, K
U	=	mean wind speed over height of plume, m/s
x	=	downwind axial distance, km
z	=	height above reference plane, m
Z	=	height of plume axis above reference plane, m
ΔZ	=	elevation of plume axis above stack top, m
Θ	=	potential temperature of ambient air, K
ρ	=	density of ambient air, kg/m^3
σy	=	standard deviation of plume spread in crosswind direction, m
σz	=	standard deviation of plume spread in vertical direction, m.

INTRODUCTION

The development of fossil-fuel reserves in remote areas of Canada in recent years has resulted in numerous research programs on the effects of on-site extraction and processing plants on the surrounding environment. In one such program, the behaviour of hot plumes from an oil-sands refinery complex in northeastern Alberta was studied by the Canada Centre for Mineral and Energy Technology (CANMET) to obtain atmospheric dispersion parameters that could be used with confidence by both energy processing industries and by environmental control authorities for optimizing stack heights and emission criteria.

This report describes 11 plume dispersion studies that were conducted during the autumn of 1971 and the winter of 1973 at an oil-sands refinery complex, about 320 km northeast of Edmonton. Atmospheric conditions ranged from stable to neutral in both seasons. Both the autumn and winter were characterized by ground-based, overnight inversions that dissipated differently because of seasonal differences in ground-cover and solar heating. In autumn, the inversion was completely dissipated by mid-day whereas in winter the inversion was only partially dissipated by sunset. On three occasions, two in autumn and one in winter, the height of the base of the inversion influenced the behaviour of the plume and resulted in a limited-mixing condition. The measured dispersion parameters are compared with those currently being used in many environmental impact studies.

DATA ACQUISITION

Emission Source Data

The oil-sands refinery complex is located at a latitude of 57°N, at the bottom of the west bank of the Athabasca River at Tar Island, 30 km north of Fort McMurray. The river at this location runs due north and the river valley is fairly shallow rising to about 275 m elevation in the west and 370 m in the east. The plant site is surrounded by coniferous forests with many open areas of muskeg.

The major sources of SO_2 emission in the refinery complex consist of a power station, incinerator, refinery and H_2S flares. At design operating

conditions, the power station consumes 2 x 10^6 kg/day of petroleum coke containing 6% sulphur and the refinery produces 2 x 10^6 gallons/day of synthetic crude oil. In the fall studies, the power station accounted for 25% of the total SO_2 emission with most of the remainder being emitted from an H_2S flare; a small amount (less than 2%) of SO_2 was emitted from a refinery flare. In winter, 80% of the SO_2 emission was from the power station with the remainder being from an incinerator stack. During both study periods, over 90% of the heat emission was from the power station stack. The heat and SO_2 emission data from the various stacks and details of the physical characteristics of these stacks are given in Tables 1 and 2 respectively. The refinery flare, H_2S flare and incinerator stack are all close together and are approximately 400 m north of the power station stack.

The Athabasca River which is 238 m above mean sea level was used as a zero altitude base line for the two study periods.

Meteorological Data

Vertical temperature and wind profiles were obtained near the plant using radiosonde and pilot balloon releases. Inaccessibility precluded the use of a remote downwind meteorological station, but the vertical temperature structure of the dispersion zone was obtained before and after each study using an instrumented helicopter.

The surface synoptic conditions for the study periods, October 4 - 8, 1971 and October 16 - 19, 1973, are shown in Figures 1 and 2 respectively.

On October 4th, a high pressure area was centred over the northwestern United States with a ridge from this system extending northwestward over central British Columbia and into the Yukon. During the next 24 hours, a low pressure area centred off of the Pacific coast moved rapidly northeastward and was centred over the Yukon by mid-day, October 5th; a warm front associated with this low pressure area extended to the southeast through central Alberta. By October 6th, the low pressure area had moved to the vicinity of Great Slave Lake with the warm front passing through central Saskatchewan and the cold front extending to the southwest of the dispersion study zone into southwestern British Columbia. By October 7th, the low pressure area had strengthened and began moving to the southeast and an area of high pressure from the Pacific had moved into east central British Columbia

and western Alberta. By mid-day of October 8th, a trough extending from a low pressure area over Alaska dominated most of northern Alberta.

With the rapidly changing synoptic pattern during this study period, the surface pressure gradient was initially strong and from the northwest ahead of the ridge, backing and becoming lighter as the ridge moved to the south.

After mid-day on October 5th, the surface gradient winds gradually changed from southerly to westerly and then to northwesterly as the Yukon low pressure area continued east and then southeastward. The strong northwesterly gradient west of this low pressure area decreased with the easterly progression of the Pacific high pressure area on October 7th. The gradient strengthened and became more westerly as a trough developed southward over Alberta by the afternoon of October 8th.

The surface temperature during the study period ranged from $2^{o}C$ to $20^{o}C$ and surface winds from 2 to 17 m/s were encountered. Atmospheric conditions ranged from stable to neutral as indicated in Table 3; an elevated inversion or limited-mixing condition was observed on two occasions.

On February 16, 1973, a low pressure area centred off the Pacific coast began to move eastward. A warm front from this low pressure area extended to the east across northern British Columbia and then to the south across central Alberta, southwest of the dispersion zone. During the evening of February 16th, the low pressure area moved rapidly to the southeast and was centred north of Fort McMurray by noon of February 17th. With passage of the low pressure area, the warm front moved north and then returned south of the dispersion zone during February 17th and 18th respectively. In the early morning of the 19th of February, another Pacific low pressure area moved inland and dominated northern Alberta; a warm front extended from it between Fort McMurray and Edmonton.

As the Pacific low pressure area moved in a southeasterly direction on February 16th, winds were light and from the southwest. The passage of the low pressure area to the northeast of the dispersion zone on February 17th was accompanied by freezing rain and overcast skies. On February 18th, as the southeasterly progression of the low pressure area continued, winds became northwesterly with snow and cloud persisting all day. By February 19th,

another Pacific low pressure area moved rapidly across northern Alberta giving clear skies and continuing light northwesterly winds.

During this study period, surface temperatures varied from -12°C to 7°C and surface winds from 1.5 m/s to 6.6 m/s. Atmospheric conditions in the dispersion zone ranged from stable to neutral. In the latter case, an elevated stable layer was present which in the majority of cases was well above the top of the plume. It, therefore, had no apparent effect on plume behaviour although, in one case, the elevated stable layer resulted in a limited-mixing condition. Table 3 gives details of the atmospheric conditions prevailing during the study periods.

Plume Dispersion Data

The procedure for the acquisition of three-dimensional plume dispersion data has been developed during a five-year field research program in various geographic regions of Canada. In this procedure, an immersion probing technique involving the deployment of a helicopter is used to measure the crosswind SO_2 and temperature profiles within the plume at two or more downwind distances and a radar positioning system is used to track continuously the helicopter. At Fort McMurray, ground-impingement profiles of SO_2 were obtained by traversing across the plume at low-altitude.

PLUME DISPERSION PARAMETERS

The detailed SO_2 and temperature distributions across the plume at two or more downwind distances were used to construct crosswind sections of the plume at those locations. Each series of crosswind sections then enabled side and plan views of the plume to be constructed. The crosswind sections were then analysed numerically to obtain the downwind distance, the plume axis elevation and the standard deviations (S.D.) of spread in the horizontal and vertical dimensions σy and σz respectively (1).

Dimensionless plume axis elevations obtained from numerical analysis and emission and meteorological parameters were derived according to the analysis of Briggs (2). This enabled comparisons between measured and empirical data to be made on a rational basis and any deviations noted.

The estimation of plume S.D.s was made by numerical analysis and the measured values were compared with the reference values of Pasquill (3). It should be noted that the curves of Pasquill, particularly for neutral conditions, are in widespread use by regulatory agencies for predictive purposes (4).

Neutral Conditions

Figure 3 shows the profiles of two of the four plumes studied under neutral conditions, one in winter and one in autumn. Typical ground-impingement SO_2 profiles are given in Figure 4.

Plume axis elevations were observed to agree reasonably well with the limiting value of Briggs. Briggs postulates that plume axis rises with downwind distance according to a 2/3-power law up to a downwind distance equivalent to about 10 stack heights. At this point where the plume axis elevation $\Delta Z = 7.4\ (h^2/L)^{1/3}$ there is no further rise of the axis, the momentum and buoyancy having dissipated in merging with the atmosphere. The measured data points, shown in Figure 5, are in this regime and tend to agree reasonably well with the predicted value of Briggs. The few points which deviate from the limiting value were probably influenced by topographic or source configuration effects not accounted for by the Briggs analysis.

A comparison of plume S.D.s in neutral conditions with those of Pasquill are given in Figure 6. In general values of σy were two classes higher than the corresponding Pasquill class for neutral condition, i.e., Class B instead of Class D. On the other hand, measured values of σz were greater close to the source but in reasonable agreement with Pasquill Class D values at downwind distances greater than 10 km. The greater initial values of σz can be attributed to source and terrain effects. The derived σy and σz values being greater than the corresponding Pasquill values strongly suggests that SO_2 concentrations at the ground are much less than would be predicted using appropriate Pasquill values for S.D.s in neutral atmospheres. There appeared to be no difference between the autumn and winter measured S.D.s in neutral conditions. A comparison of measured and calculated ground-level SO_2 levels in neutral conditions is given in Table 4. Calculated values are modified to account for the $2\frac{1}{2}$-second response time of the SO_2 analyses (5).

Stable Conditions

Figure 7 shows two of the four plumes studied during stable conditions, one in winter and one in autumn. As expected, there were no significant ground-impingement SO_2 profiles during stable conditions. The side views, which show the tendency of the stable plumes to follow rather than to impinge on the terrain, confirm the observations reported previously (6, 7, 8, 9, 10). This tendency of plumes to remain buffered by a thin layer of stable air adjacent to the ground, coupled with the poor dispersive capacity of the stable atmoshphere, will minimize ground impingement.

Briggs predicted a levelling-off of the plume axis at a dimensionless downwind distance greater than $X = 2.4US^{-\frac{1}{2}}$. The limiting value of dimensionless plume axis elevation of 2.9 is shown in Figure 8 together with the measured values. It must be noted that none of the data utilized by Briggs exceeded a dimensionless downwind distance of 7 and the values used in these studies ranged from 10 to 550. An examination of the measured data reveals that the plume axis has a tendency to rise to a maximum value and then as its buoyancy and momentum are dissipated to fall back to zero. This finding has been observed during plume dispersion studies elsewhere in Canada and during other studies at the same plant (6, 8, 11).

As shown in Figure 9, measured σy values during stable conditions were higher by an order of magnitude than the corresponding Pasquill curve. In general, these σy values agreed more with Pasquill Class A, the most unstable atmospheric condition, rather than with Class F, the most stable. There appeared to be no difference in horizontal spread in the autumn and winter studies. However, there was a significant difference in vertical spread between the autumn and winter studies. The regression lines in Figure 9 show that the measured values of σz in the autumn studies were significantly lower than those of the winter studies. In both cases, the slope of the regression line was much less than the Pasquill Class F curve, being almost zero. This finding indicates that vertical S.D. was essentially constant with downwind distance during both the autumn and winter studies. An examination of plume S.D.s in stable conditions clearly indicates that SO_2 concentrations within the plume would be much less than predicted by Pasquill values and that the potential for severe daytime fumigations is significantly reduced. In addition, there was no significant impingement of the stable

plumes on the gradually rising terrain on either side of the river valley.

Limited-Mixing Conditions

A limited-mixing condition occurs when the plume is constrained within an atmospheric layer that is capped by another layer of different stability. Usually the dispersion layer is neutral or isothermal and the elevated layer is more stable. However, experience has also shown that a plume may become embedded in a stable layer beneath an elevated neutral layer. A general conclusion is that plumes have a natural reluctance to disperse beyond the layer into which they are emitted, unless buoyancy and momentum forces overcome this reluctance. Figure 10 shows two of the three plumes which were studied during limited-mixing conditions. Ground impingement SO_2 profiles are given in Figure 11.

In both of the autumn studies, the plume was embedded in an isothermal layer which was capped by a very strong thin inversion having a potential temperature gradient greater than $6^{\circ}C/100$ m and a total thickness of about 75 m. However, in the winter study, the neutral dispersion layer was under an elevated inversion that had a temperature gradient of only $1.66^{\circ}C/100$ m and a thickness of 600 m. In general, the strength or thickness of the elevated inversion layer should have little influence on plume axis elevations, if upward dispersion of the plume is unrestricted. On the other hand, elevated inversions based at low altitudes that are either strong and thin or weak and thick will tend to prevent plume penetration.

Figure 12 shows dimensionless plume axis elevations plotted against downwind distance for the studies carried out during winter and autumn when limited-mixing conditions prevailed. In all three cases, the plume was observed to become trapped below its limiting value. The limiting value is a direct function of the space available for dispersion between the stack top and the base of the inversion (12). The initial penetration of the strong inversion during the autumn is probably due to initial buoyancy and momentum effects and the close proximity of the inversion base to the stack top. In this case, initial source momentum and buoyancy has not been destroyed by atmospheric dilution and some deflection of the inversion base will likely result.

Figure 13 shows that the measured values of σy corresponded to Pasquill Class B, whereas the prevailing atmospheric stabilities corresponded

to Pasquill Class D in autumn and Class E in winter. Again, similar to the neutral and stable studies, there was no apparent difference between winter and autumn σy values.

Measured σz values were almost constant with downwind distance because of the restriction of vertical dispersion by the inversion base. For this reason vertical S.D. does not enter into the atmospheric dispersion model for limited-mixing conditions. Since limited-mixing conditions provide the greatest potential for plume impingement with the ground, it is clear that the greater measured σy values resulted in lower concentrations of stack gases over the ground than would be obtained by using Pasquill values. This finding is illustrated in Table 4, in which measured SO_2 concentrations for the same sampling time for limited-mixing conditions are observed to be much less than those calculated by using Pasquill.

CONCLUSIONS

The behaviour of 11 plumes from an oil-sands refinery complex located in northeastern Alberta under a range of meteorological conditions shows that:

(1) Plume axis elevations were in good agreement with the limiting-value suggested by Briggs for neutral conditions. In stable conditions, the plume axis, after its initial rise, had a tendency to return to zero at downwind distances greater than 30 km. This phenomenon is not indicated by the Briggs' equation for stable conditions, possibly because of the unavailability of measured values at such large downwind distances. Under limited-mixing conditions, the plume levelled off at a limiting value which depended on the available mixing height.

(2) The measured values of horizontal S.D., σy, were higher than the corresponding values of Pasquill under neutral, stable and limited-mixing conditions. In neutral conditions the difference was two stability classes, Class B rather than Class D; in stable conditions six stability classes, A rather than F. It is important to note that Class F is the most stable Pasquill stability category and that some of the

stabilities measured would be much more stable than this arbitrary classification would allow. In limited-mixing conditions, the values of σy corresponded to Class B instead of Class E, but this can be expected when vertical dispersion is restricted by the elevated stable layer.

(3) Measured values of vertical S.D., σz, in general agreed with Pasquill values in neutral conditions at downwind distances between 8 - 40 km. Closer to the source, values were higher than Pasquill, possibly because of source and terrain effects; however, it is unlikely that these values would unduly influence ground impingement profiles because of their proximity to the point of emission. In stable conditions, there was a significant difference between σz values measured during autumn and winter. Winter values were higher and corresponded to Pasquill Class F from 8 - 60 km downwind. Those σz values measured in autumn corresponded to Pasquill Class F between 3 and 8 km downwind. However, many of the stable study periods corresponded to a classification more stable than Pasquill Class F (Table 3). Measured values of σz under limited-mixing conditions levelled off according to the available space for dispersion in the same manner as the plume axis elevation.

(4) It is clear, from an examination of the degree of dispersion and the ground-impingement SO_2 concentrations measured during the studies, that the corresponding values estimated using Briggs and Pasquill were significantly higher. Such field studies can provide valuable input data for modelling economic costs and energy penalties associated with pollution control measures such as emission levels, stack heights, exit gas temperature and pollutant removal.

ACKNOWLEDGEMENTS

The plume dispersion studies at Fort McMurray were conducted with the cooperation and technical support of Great Canadian Oil Sands Ltd. (G.C.O.S.).

Meteorological support and forecasting were provided by the Atmospheric Environment Service of Environment Canada.

The cooperation of Alberta Environment and the Alberta Energy Resources Conservation Board was greatly appreciated.

The plume dispersion research program is conducted jointly with industry and is part of the conservation segment of the Energy Program of the Canada Centre for Mineral and Energy Technology (CANMET).

REFERENCES

1. Whaley, H. The derivation of plume dispersion parameters from measured three-dimensional data; Atmospheric Environment; v. 8, pp 281-290; 1974.

2. Briggs, G.A. Plume rise; U.S.A.E.C. TID 25075, 81 p; 1969.

3. Pasquill, F. Atmospheric diffusion; D. Van Nostrand Co. Ltd.; ch. 5, pp 179-214; 1968.

4. Turner, D.B. Workbook of atmospheric dispersion estimates; U.S.D.H.E.W., P.H.S.P.; no. 999-AP-26; 1969.

5. Hino, M. Maximum ground-level concentration and sampling; Atmospheric Environment; v. 2, pp 149-165; 1968.

6. Whaley, H. and Lee, G.K. Plume dispersion from a thermal power station on the shore of a large lake; J. Inst Fuel; v. 47, pp 242-250; 1974.

7. Whaley, H. and Lee, G.K. Plume dispersion in a mountainous river valley during spring; accepted for publication; J. Air Pollution Control Association; 1976.

8. Whaley, H. and Lee, G.K. An assessment of plume dispersion parameters measured in fall and winter at a tar-sands refinery complex; in preparation for the 70th annual meeting of the Air Pollution Control Association; June 1977.

9. Shenfield, L., Hirt, M.S., Whaley, H. and Lee, G.K. Diffusion studies of plumes influenced by an urban area and a large relatively cold lake; paper B.16, proceedings 3rd International Clean Air Congress; Oct. 1973.

10. Leahy, D.M. and Rowe, R.D. Observational studies of atmospheric diffusion processes over irregular terrain; 67th annual meeting; Air Pollution Control Association; paper 74-67; 1974.

11. Whaley, H. and Lee, G.K. Plume dispersion from a lignite-fired power station in flat, rural terrain; A.S.M.E., winter annual meeting; paper no. 76-WA/APC-7; Dec. 1976.

12. Whaley, H., Lee, G.K. and Gainer, J. Plume dispersion from a natural gas sulphur extraction plant under a persistent elevation inversion; 13th World gas conference; June 1976.

TABLE 1. Emission Source Data

		Power Station		Incinerator		Refinery Flare		H_2S Flare	
Date	Time MST	Heat Emission MW	SO_2 Emission sm^3/s	Heat Emission MW	SO_2 Emission sm^3/s	Heat Emission MW	SO_2 Emission sm^3/s	Heat Emission MW	SO_2 Emission sm^3/s
4-10-71	1504-1618	69.97	0.63	-	-	2.09	0.04	0.54	1.59
5-10-71	0724-0821	66.70	0.63	-	-	2.11	0.04	0.54	1.55
6-10-71	0710-0758	65.09	0.33	-	-	1.10	0.04	0.28	0.76
7-10-71	1102-1200	74.71	0.33	-	-	2.68	0.04	0.68	2.04
8-10-71	0702-0845	80.91	0.33	-	-	2.29	0.04	0.59	1.75
8-10-71	0941-1140	80.02	0.33	-	-	2.29	0.04	0.59	1.82
16-2-73	1402-1557	86.51	0.53	9.28	0.15	-	-	-	-
17-2-73	0849-1034	82.06	0.53	9.26	0.11	-	-	-	-
17-2-73	1419-1627	84.22	0.53	9.04	0.11	-	-	-	-
19-2-73	0830-1009	81.41	0.52	9.68	0.13	-	-	-	-
19-2-73	1308-1449	93.37	0.53	10.01	0.13	-	-	-	-

TABLE 2. Physical Characteristics of Stacks

Stack	Height m	Diameter m	Base Elevation above Mean Sea Level, m
Power Station	106	5.89	362.7
Incinerator	106	1.61	363.4
Refinery Flare	106	0.91	350.5
H_2S Flare	75.7	0.46	320.0

TABLE 3. Atmospheric Conditions During the Study Periods

Date	Time MST	Mean Wind		Ambient	∂Θ / ∂Z	Height	Atmospheric Stability	
		Speed m/s	Direction deg	Temp (Stack Top) °C	°C/100 m	Interval m	Thermal Regime	Pasquill Class
4-10-71	1504-1618	7.0	293.9	16.5	0.04	0-900 *	Neutral	D
5-10-71	0724-0821	2.5	236.8	6.6	0.66	0-120	Isothermal	E
					3.81	120-400 *	Inversion	F+
6-10-71	0710-0758	6.5	190.6	10.2	4.41	0-300 *	Inversion	F+
7-10-71	1102-1200	10.9	312.3	8.6	-0.37	0-1400*	Neutral	C/D
8-10-71	0702-0845	5.8	192.7	2.6	1.00	0-280 *	Isothermal	E
					6.17	280-350	Inversion	F+
					0.65	350-1400	Isothermal	E
8-10-71	0941-1140	7.3	201.3	5.8	1.00	0-400 *	Isothermal	E
					6.02	400-480	Inversion	F+
					0.48	480-1400	Neutral	D/E
16-2-73	1402-1557	4.6	328.3	2.3	0.45	0-1200*	Neutral	D/E
17-2-73	0849-1034	8.3	220.1	1.5	3.72	0-500 *	Inversion	F+
					0.49	500-1200	Neutral	D/E
17-2-73	1419-1627	9.2	278.7	6.1	3.81	0-180 *	Inversion	F
					1.00	180-425 *	Isothermal	E
					0.29	425-1200*	Neutral	D
19-2-73	0830-1009	4.3	344.2	-11.5	1.37	0-1300*	Isothermal	E
19-2-73	1308-1449	4.0	0.7	-11.5	0.40	0-500 *	Neutral	D/E
					1.66	500-1100*	Inversion	F

*Dispersion Zone

TABLE 4. Comparison of Predicted and Measured Maximum Ground-Impingement SO_2 Concentration

Date	Time MST	Atmospheric Condition	Distance From Plant km	Predicted SO_2 / Measured SO_2
4-10-71	1504-1618	Neutral	1.3*	-
			4.6*	-
			15.2	14.1
7-10-71	1102-1200	Neutral	2.8	2.5
			6.1	5.3
			15.4	12.5
8-10-71	0702-0845	Limited-mixing	3.7	125.0
			18.6	34.0
			34.0	335.0
8-10-71	0941-1140	Limited-mixing	1.1	413.5
			18.1	34.7
			31.8	21.5
			46.7	11.2
16-2-73	1402-1557	Neutral	3.4	0.0
			16.7	0.8
			22.6	2.2
17-2-73	1419-1627	Neutral	2.8*	-
			5.2	1.5
			9.9	9.0
19-2-73	1308-1449	Limited-mixing	4.8*	-
			15.8	24.0
			27.9	11.5

*No SO_2 measured at ground-level.

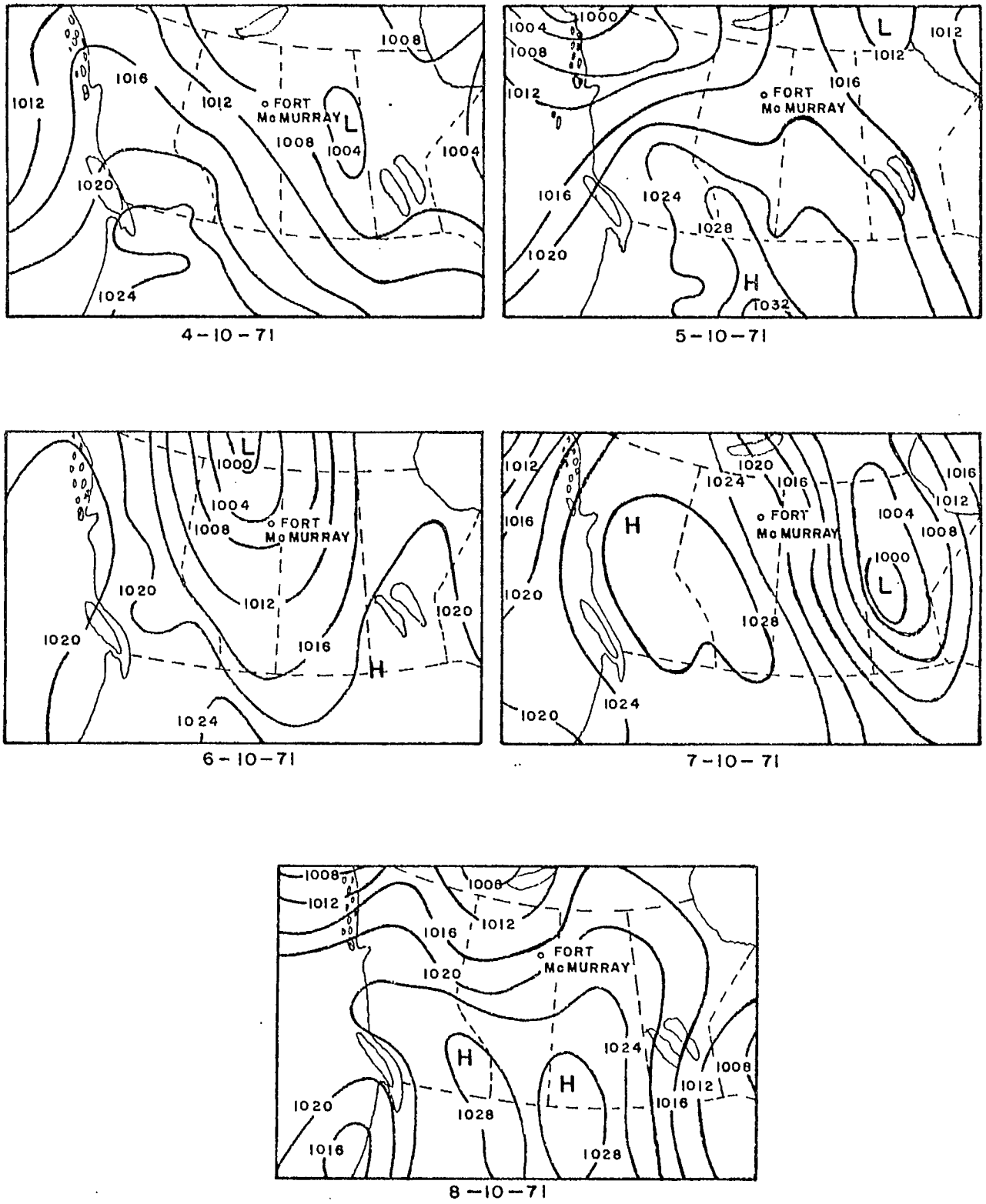

FIGURE 1 Synoptic surface weather maps 1100 MST October 4-8, 1971

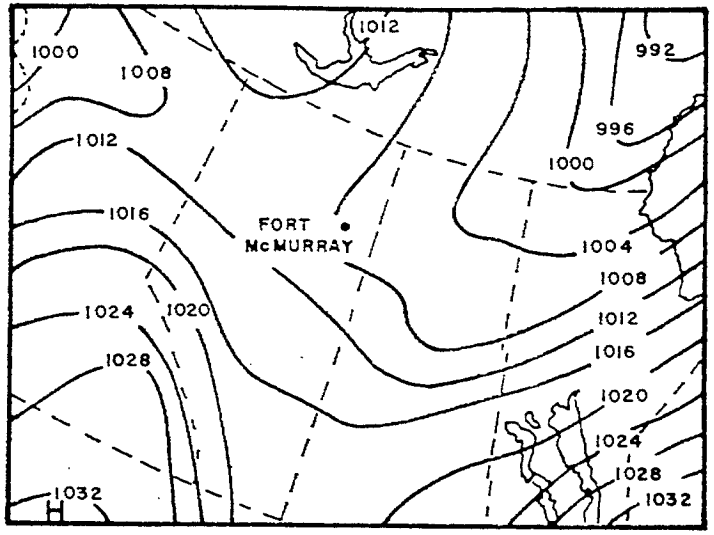

16-2-73

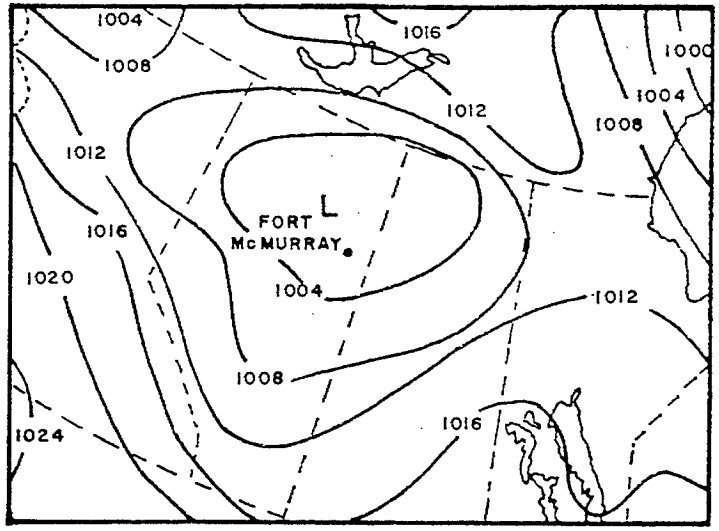

17-2-73

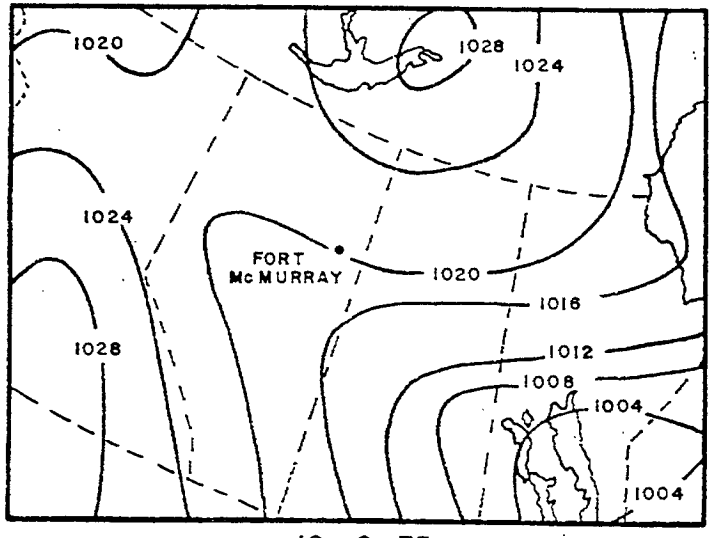

18-2-73

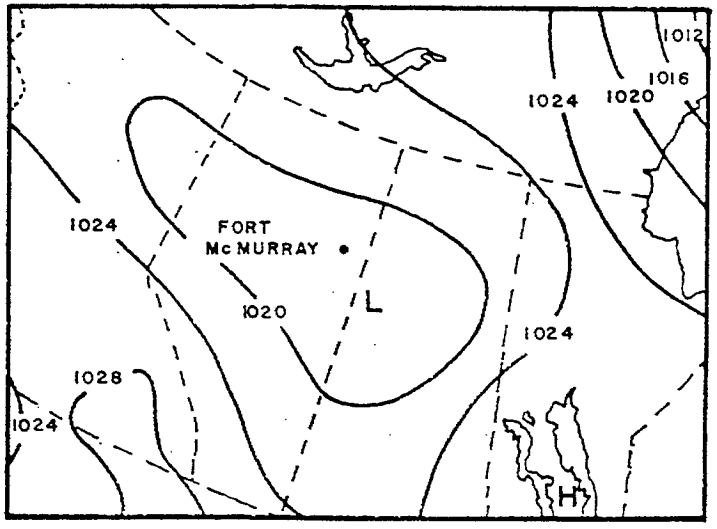

19-2-73

FIGURE 2 Synoptic surface weather maps 1100 MST February 16-19, 1973

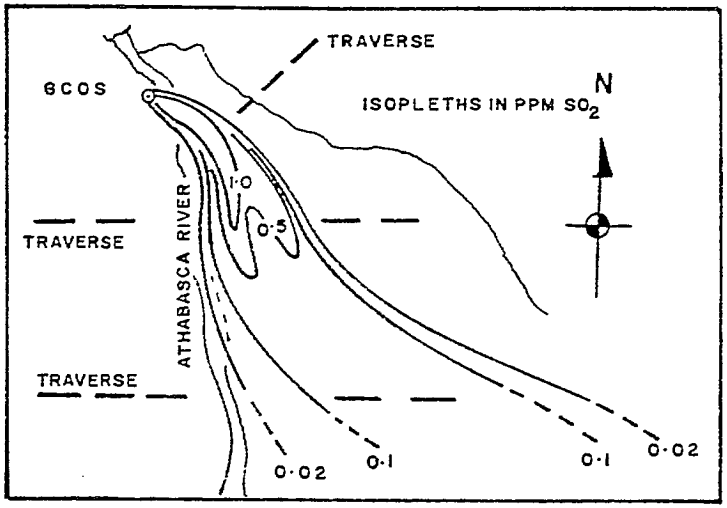

PLAN VIEW

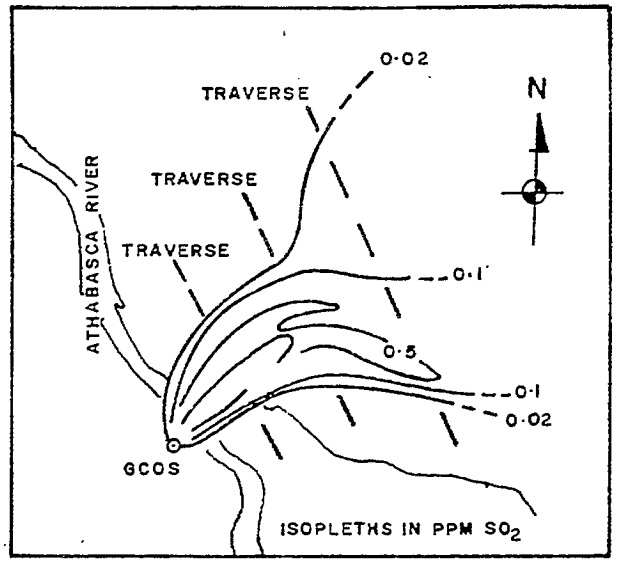

PLAN VIEW

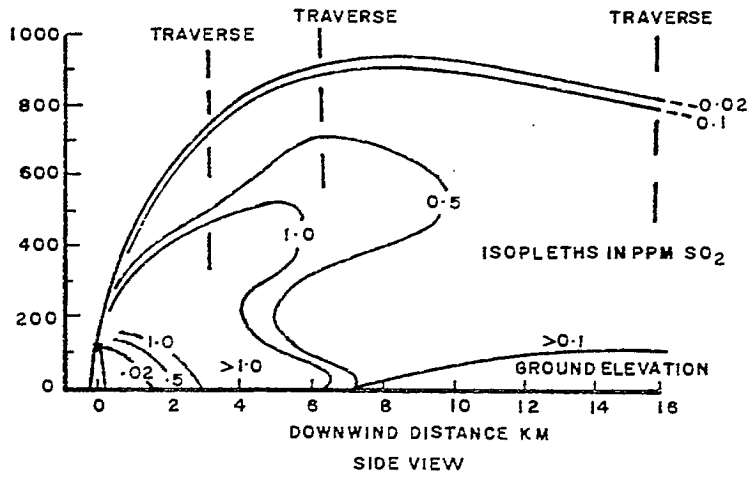

SIDE VIEW

7-10-71, 1102-1200 MST

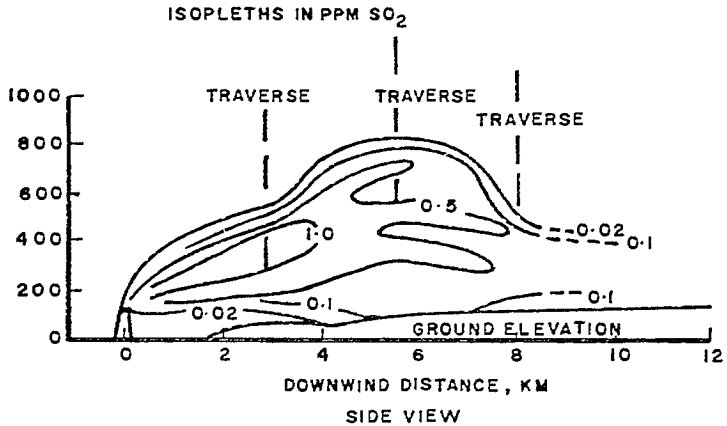

SIDE VIEW

17-2-73, 1419-1627 MST

FIGURE 3 Plan and side views of typical plumes in neutral conditions

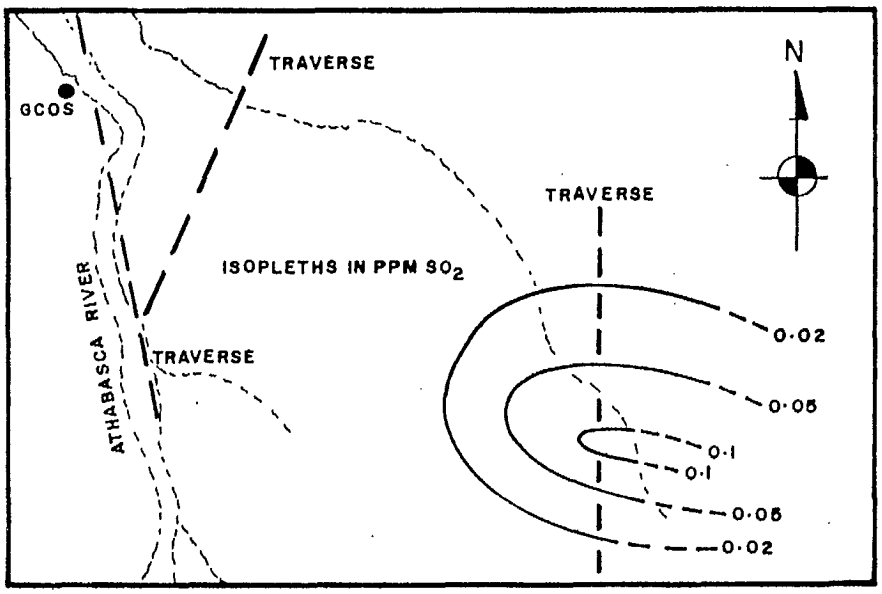

4-10-71, 1504-1618 MST

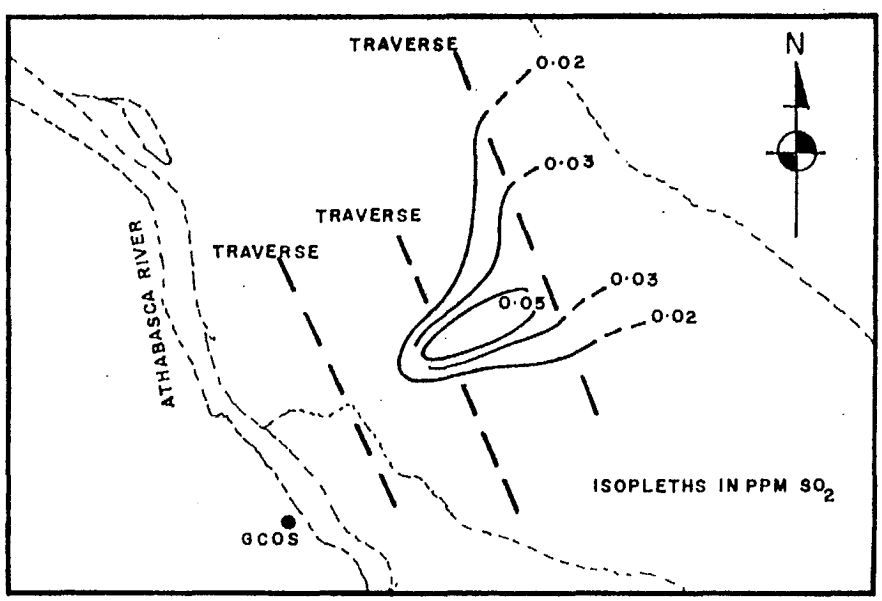

17-2-73, 1419-1627 MST

FIGURE 4 Ground-impingement SO_2 profiles in neutral conditions

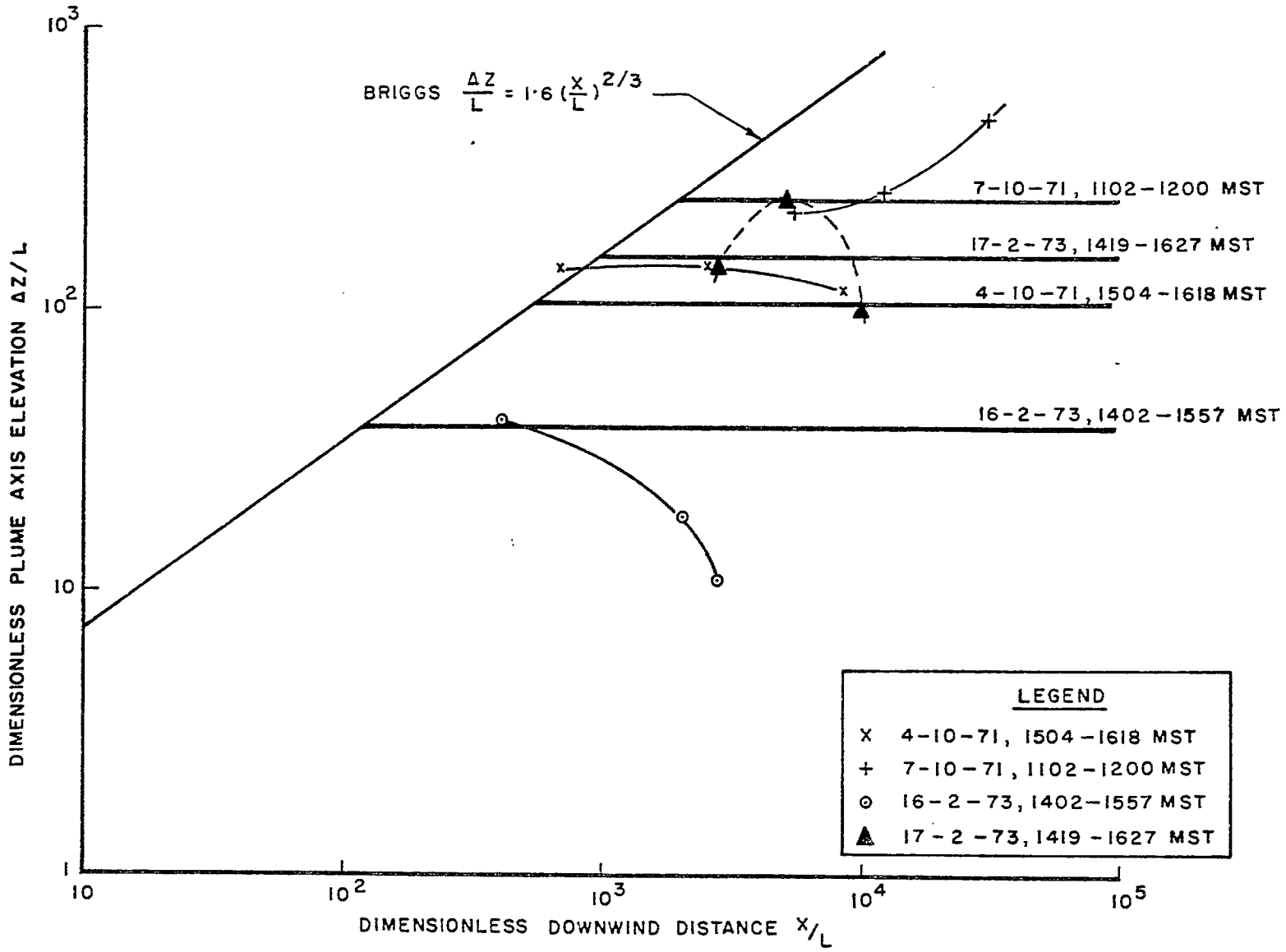

FIGURE 5 Plume axis elevation during neutral conditions; horizontal lines represent the Briggs limiting value

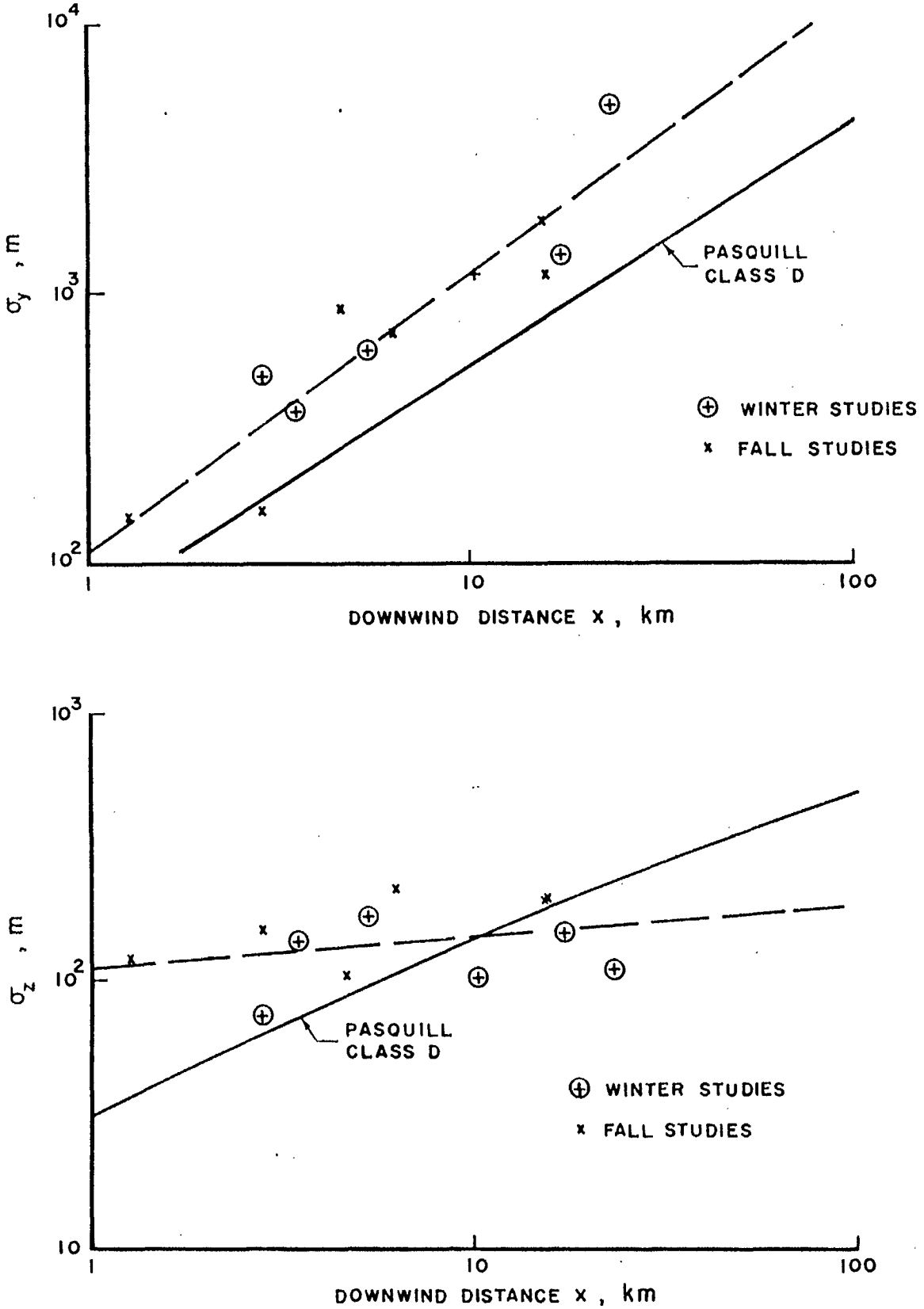

FIGURE 6 Plume S.D.s during neutral conditions; broken lines represent best-fit regression lines

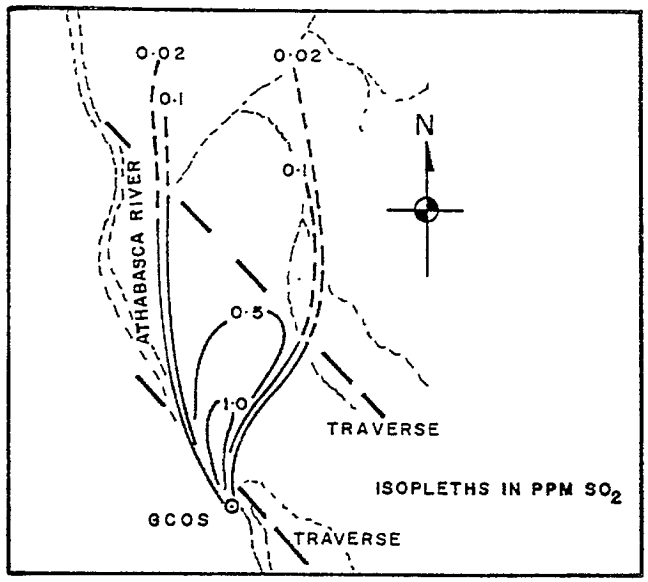

PLAN VIEW

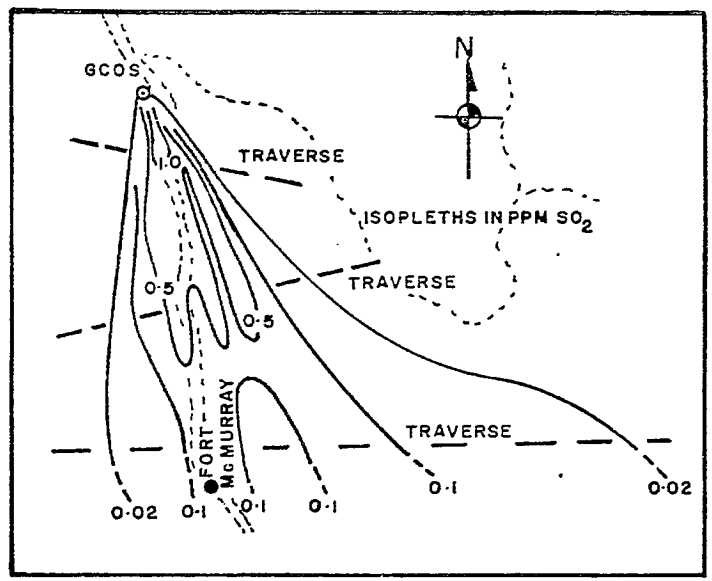

PLAN VIEW

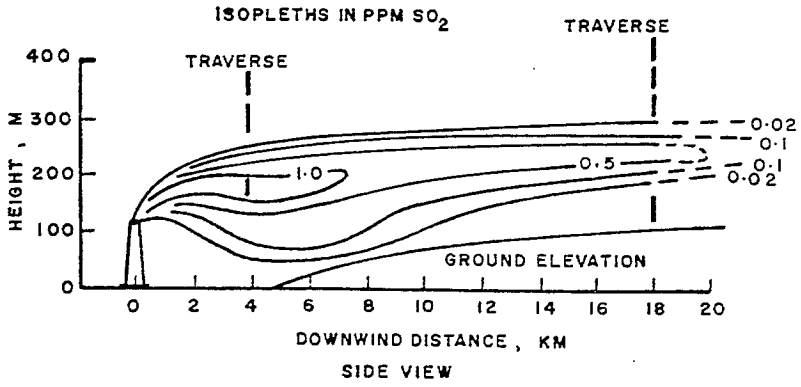

SIDE VIEW

6-10-71, 0710-0758 MST

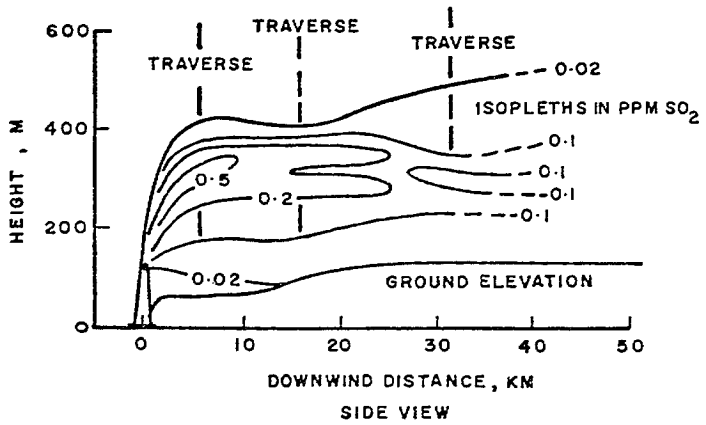

SIDE VIEW

19-2-73, 0830-1009 MST

FIGURE 7 Plan and side views of typical plumes in stable conditions

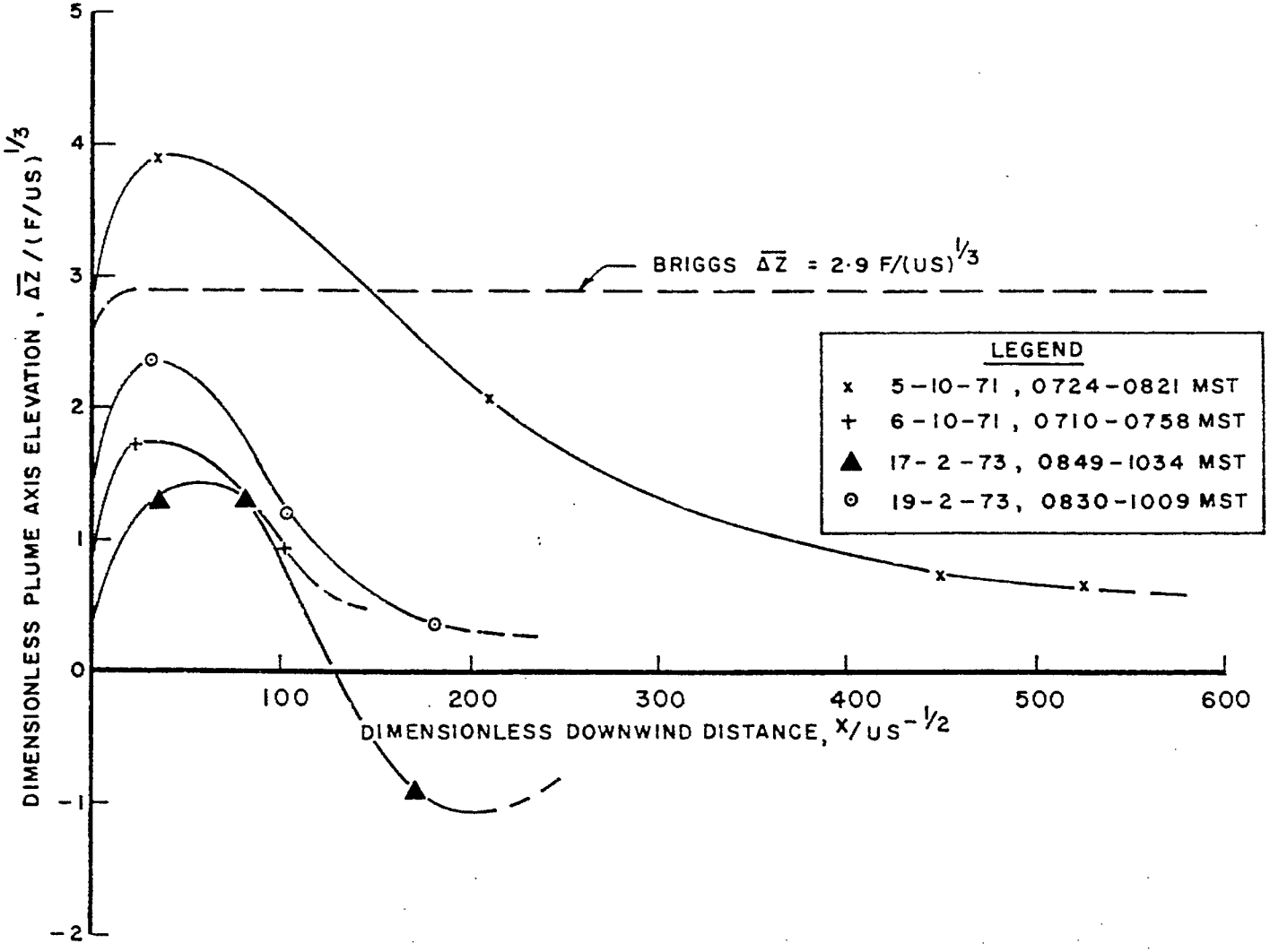

FIGURE 8 Plume axis elevations during stable conditions; horizontal line represents the Briggs limiting value

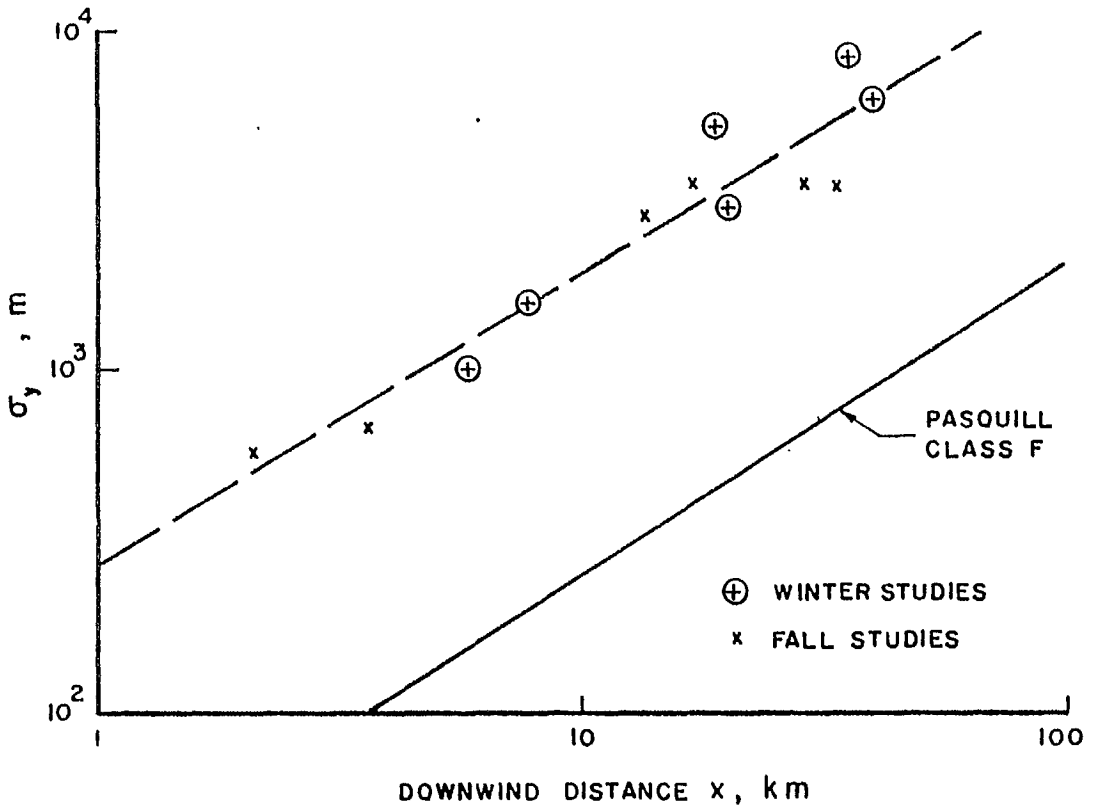

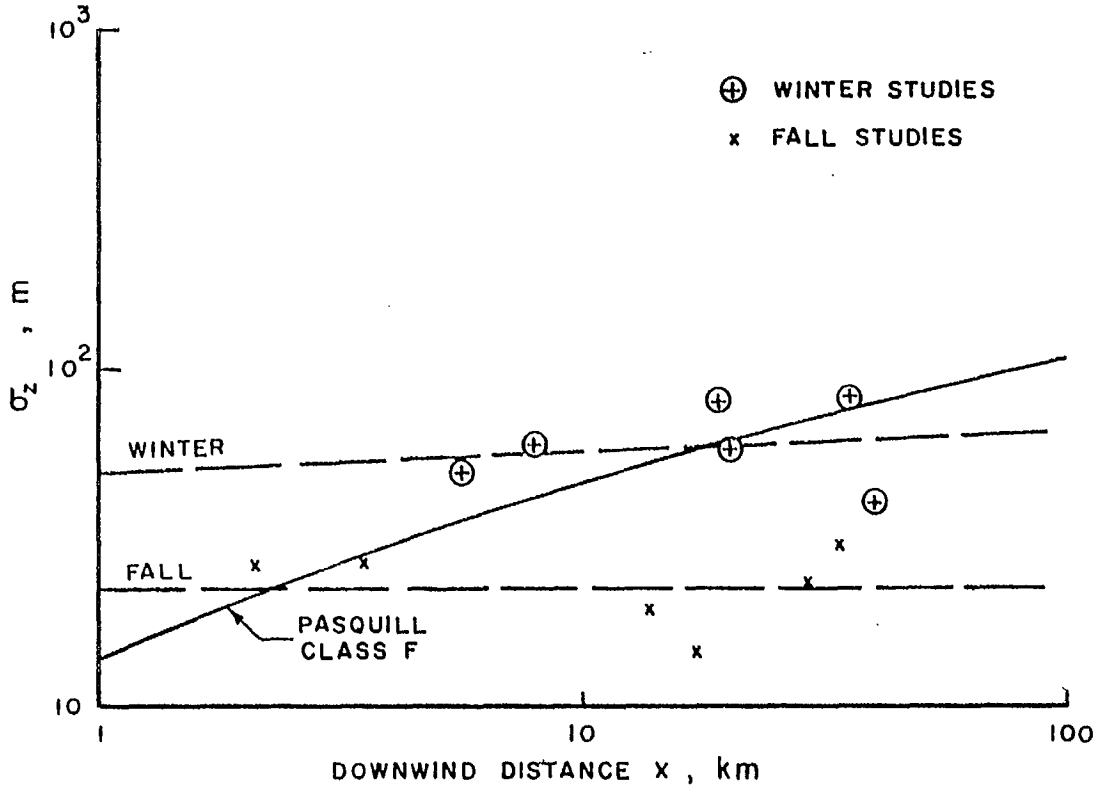

FIGURE 9 Plume S.D.s during stable conditions; broken lines are best-fit regression lines

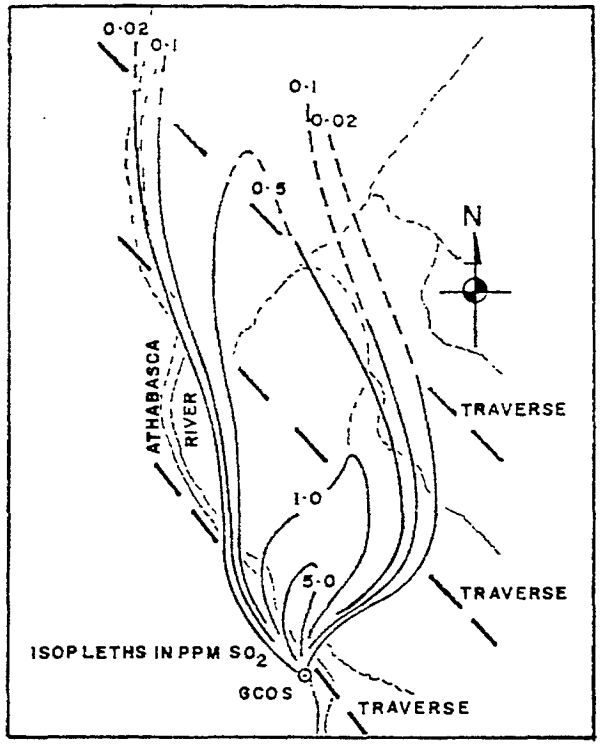

PLAN VIEW

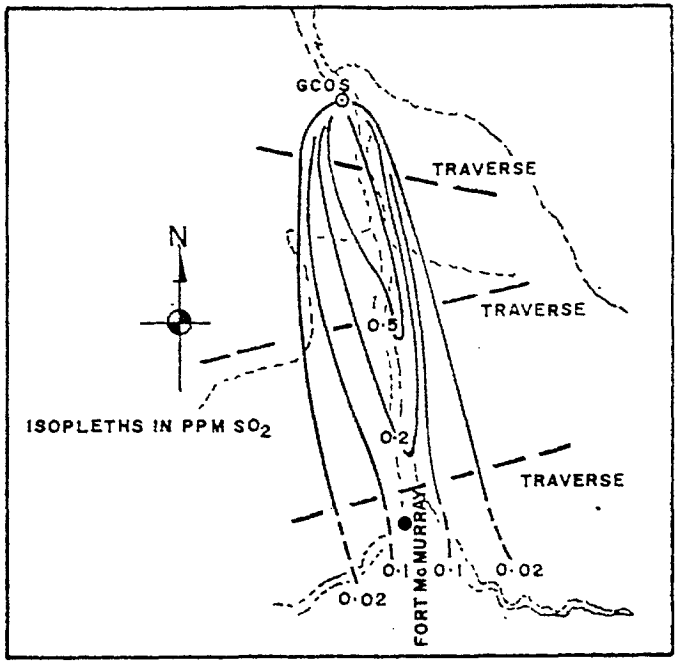

PLAN VIEW

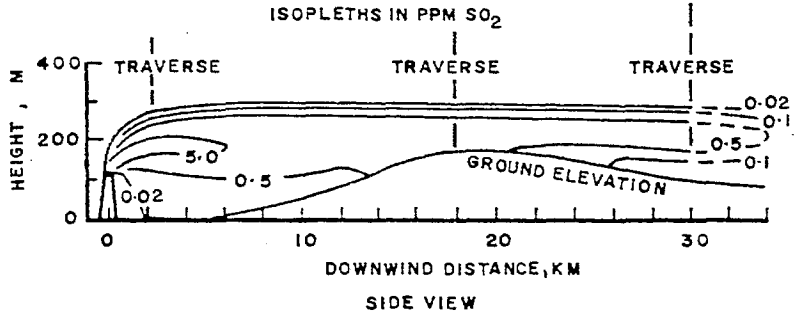

SIDE VIEW

8-10-71, 0702-0845 MST

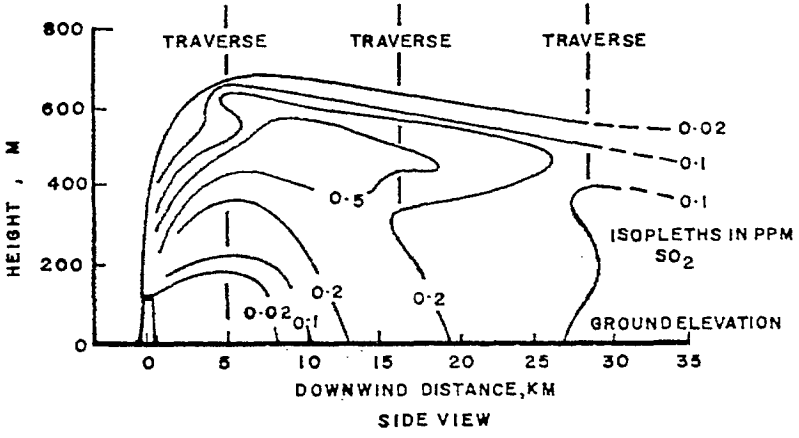

SIDE VIEW

19-2-73, 1308-1449 MST

FIGURE 10 Plan and side views of typical plumes under limited-mixing conditions

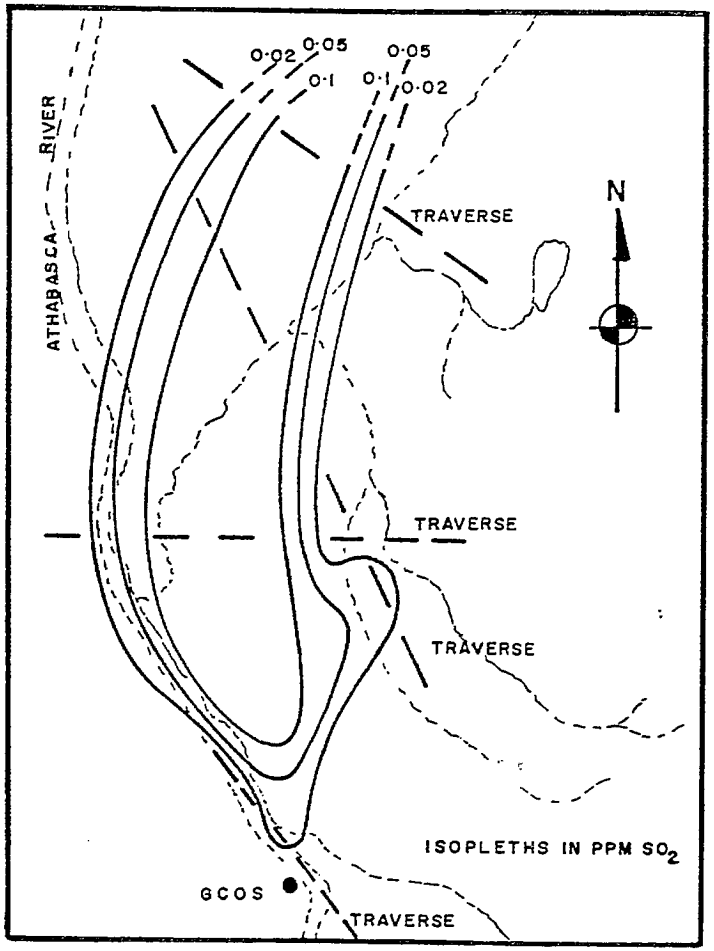

8-10-71 0941-1140 MST

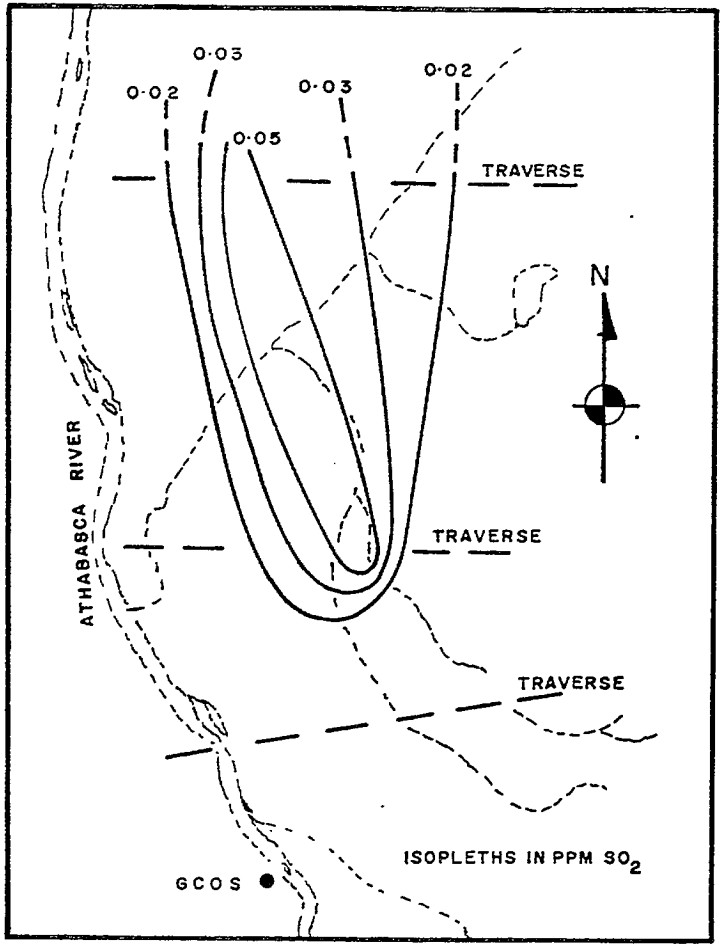

17-2-73 0849-1034 MST

FIGURE 11 Ground-impingement SO_2 profiles under limited-mixing conditions

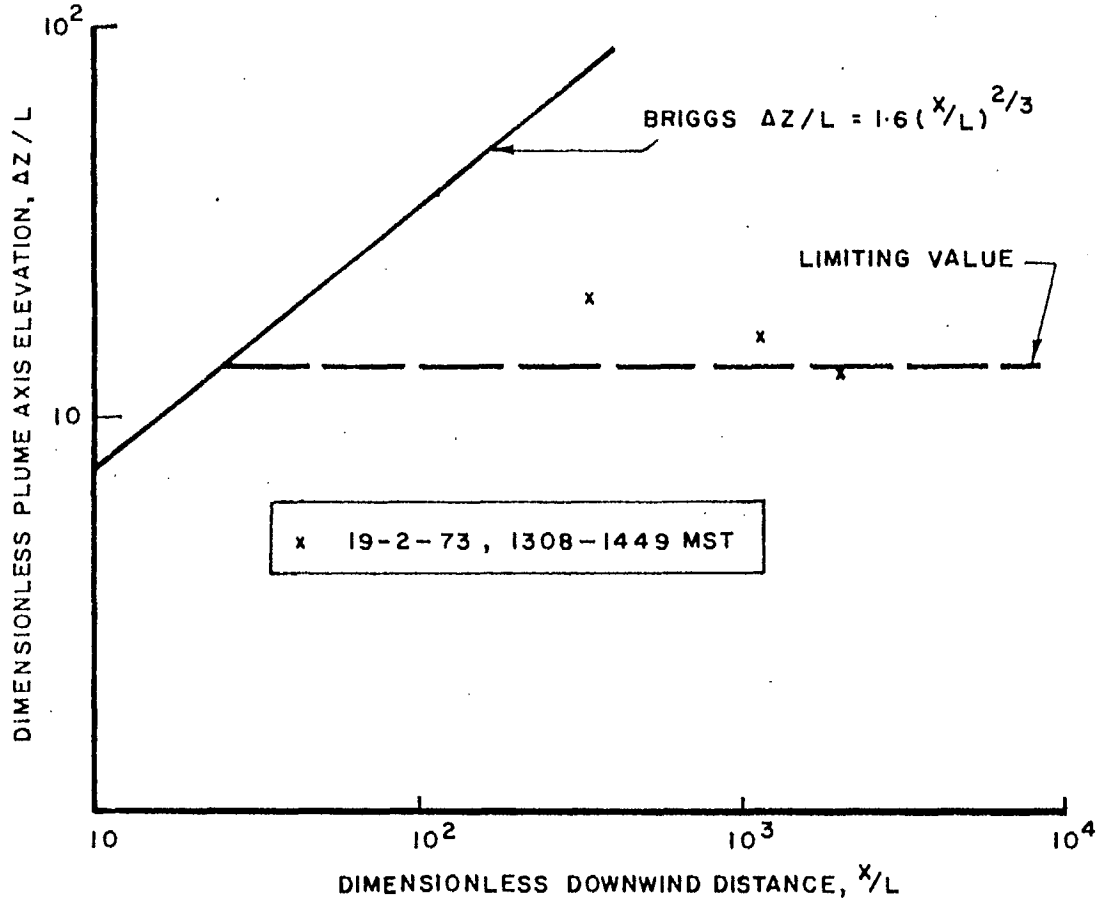

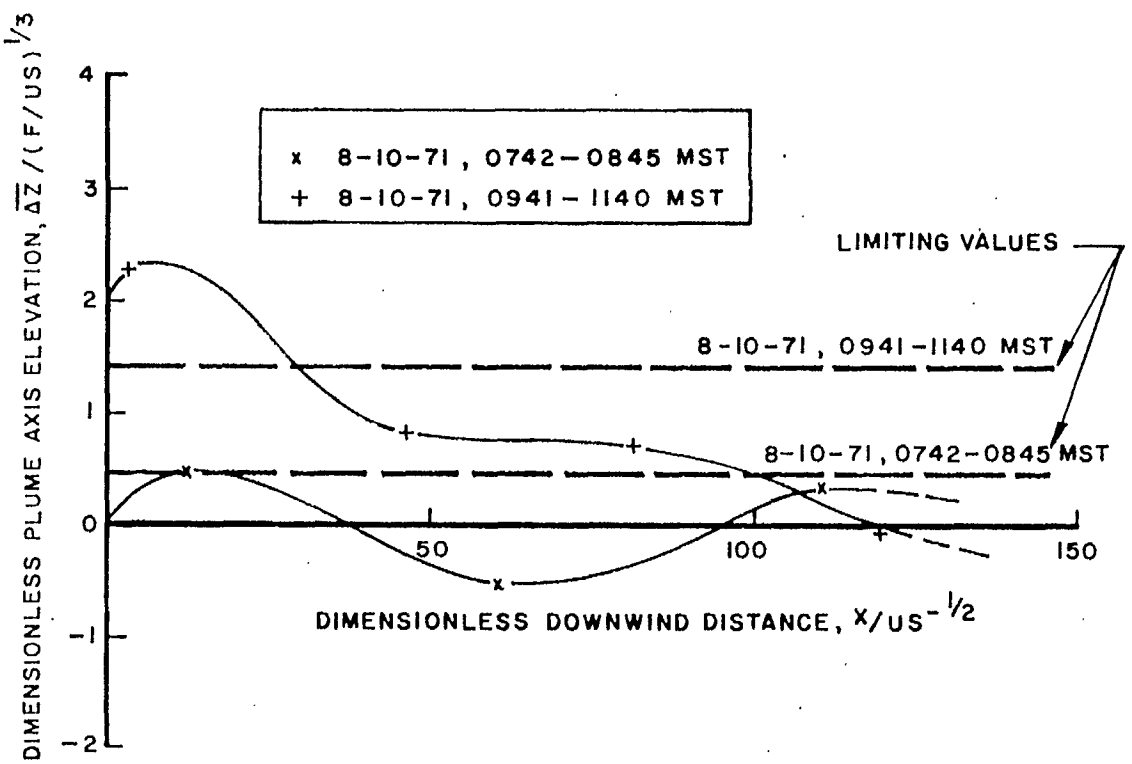

FIGURE 12 Plume axis elevations under limited-mixing conditions; horizontal lines represent limiting values

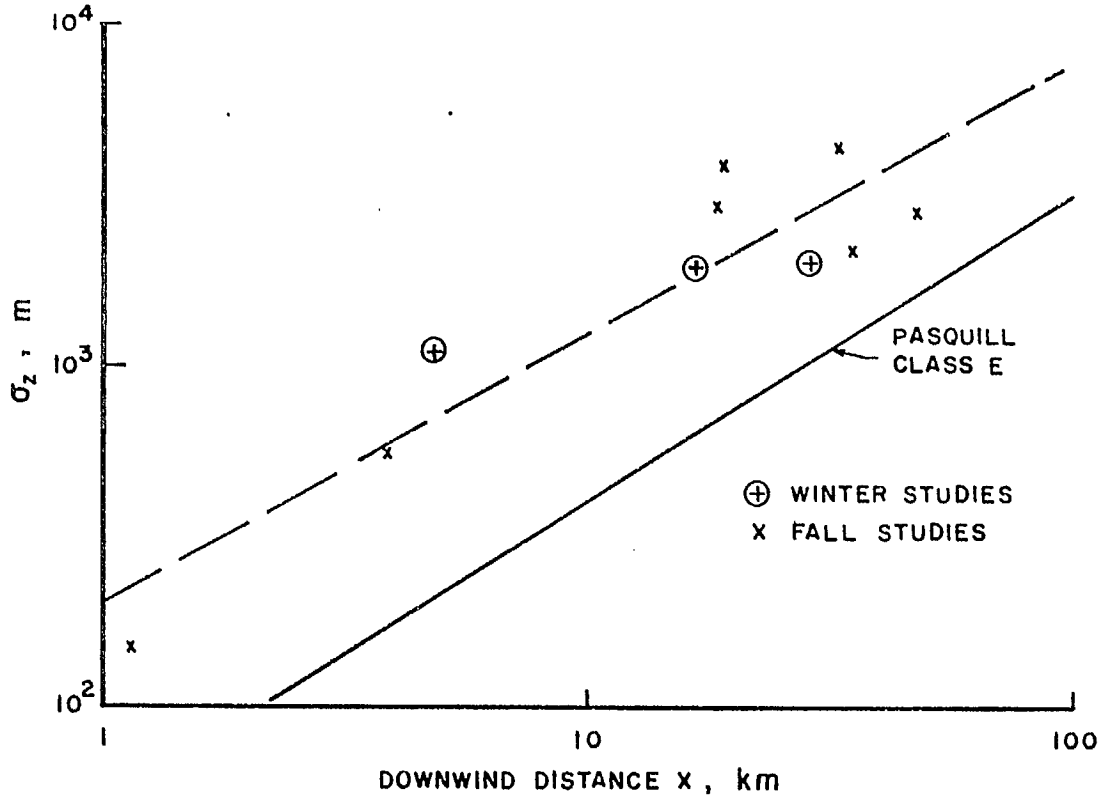

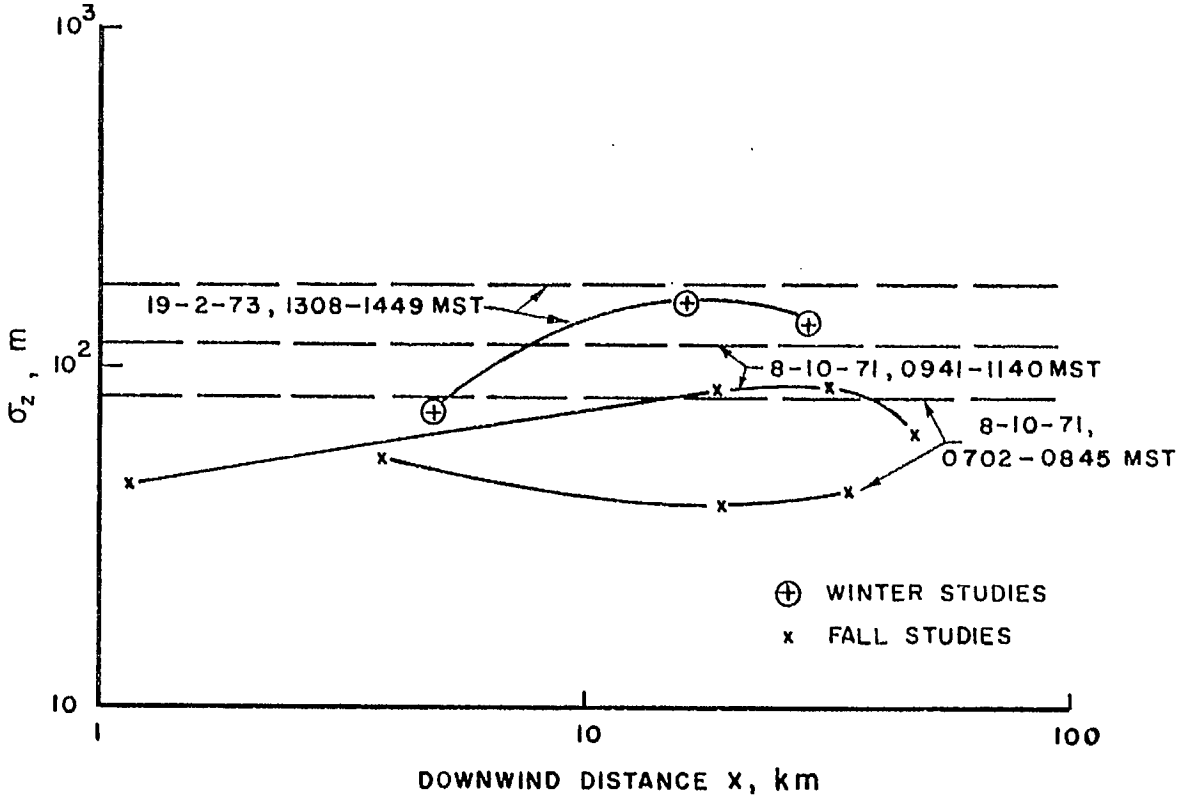

FIGURE 13 Plume S.D.s under limited-mixing conditions; horizontal lines represent limiting values